Aerosol and Air Quality Research, 16: 1991–2002, 2016

ISSN: 1680-8584 print / 2071-1409 online
doi: 10.4209/aaqr.2015.11.0645

Numerical Study of Reverse Multi-Pulsing Jet Cleaning for Pleated Cartridge Filters

Shaowen Chen[1,2], Da-Ren Chen[2*]

[1] *School of Energy Science and Engineering, Harbin Institute of Technology, Harbin, Heilongjiang 150001, China*
[2] *Particle Lab, Department of Mechanical and Nuclear Engineering, Virginia Commonwealth University,401 West Main Street, Richmond, VA 23294, USA*

ABSTRACT

Patchy cleaning is one of issues often encountered for pleated filter cartridges (in an industrial filtration system) undergoing the reverse flow cleaning for filtration medium regeneration. To improve the cleaning quality for pleated filter cartridges, a novel reverse multi-pulsing jet cleaning was introduced in this study. A CFD modeling, via ANSYS CFX R.14, was applied to study the time-dependent flow and pressure fields in a simple filtration system with one filter cartridge under the proposed reverse flow cleaning. The transient static pressure fields for pleated cartridges under the cleaning with four flow pulsing waveforms and three pulsing frequencies were investigated. Cartridges with triangular pleats were selected as the model cartridge. It was found that the reverse multi-pulsing jet operation was able to effectively improve the cleaning performance without the increase of compressed gas tank pressure. The studied operation increased the number of cleaning action and local acceleration at the top sections of filter cartridges. In addition, the surface-averaged peak pressure drop across pleated filter media at the base section of cartridges was also 6.5% increased when pleated cartridges were cleaned by the proposed scheme as compared to that cleaned by the single-pulsing flow scheme. The peak pressure drop increase enhanced the cleaning mechanical stress at the base section of cartridges. The better performance for reverse flow cleaning was found in the multi-pulsing mode having the rectangular waveform and at high frequency. The observed peak pressure drop increase at the base section of filters was found closely related to the interaction of residual gas from the former pulsing and jet flow from the later pulsing. Further investigation indicated that the observed cleaning performance improvement was also shown under the consideration of the tank pressure reduction and change of media permeability during the removal of dust cake built-up on filter surface.

Keywords: Pleated filter cartridge; Multi-pulsed jet; Pulse waveform; Reverse pulsed-jet cleaning.

INTRODUCTION

Filtration systems with filter cartridges have been utilized in industrial applications for either removing particulate matter (PM) or recovering powders from industrial processes. As PM continues being collected on the surfaces of filter cartridges during the filtration the cartridge pressure drop increases (Novick *et al.*, 1992; Cheng and Tsai, 1998). Periodical regeneration of filter cartridges is then required for continuously operating filtration systems. Regeneration of filter cartridges is typically accomplished by a reverse flow cleaning, especially when collecting dry PM. Filtration efficiency and lifetime of filter cartridges are greatly influenced by the cleaning via injecting a high-pressure jet flow (in the reverse filtration flow direction) in the direction reverse to that of filtration flow for a very brief duration (Leith and Ellenbecker, 1980; Chen and Pui, 1996; Calle *et al.*, 2002; Binnig *et al.*, 2009). The research and development of an effective reverse pulsing-jet cleaning process are thus important for industrial filtration applications.

Several factors are expected to have an effect on the cleaning efficiency of pleated filter cartridges. They include the pleat geometry (Lo *et al.*, 2010a, b), compressed gas tank pressure and pulse duration (Lo *et al.*, 2010a, b; Li *et al.*, 2015), injection nozzle (Yan *et al.*, 2013; Qian *et al.*, 2014; Li *et al.*, 2015; Yan *et al.*, 2015), cleaning mode (Lo *et al.*, 2010a), cone installation (Li *et al.*, 2015), clogging of filter media (Calle *et al.*, 2004), and particle types (Bemer *et al.*, 2013). Research (Lu and Tsai, 1996; Ji *et al.*, 2004; Simon *et al.*, 2007; Park *et al.*, 2012) has been performed to improve the cleaning performance during a reverse pulsing-jet process for baghouse and filter cartridges.

Under the action of a high-speed jet flow initiated from an injection nozzle, it is believed that local mechanical

* Corresponding author.
Tel.: 1-804-828-2828; Fax: 1-804-827-7030
E-mail address: dchen3@vcu.edu

stress distribution on the filter surface plays a major role in the cleaning process. Non-uniform cleaning (i.e., patchy cleaning) and significant pressure variation in reverse flow cleaning process remain as issues in industrial filtration systems. It is because that they often result in adverse effect on the cleaning efficiency/quality and lifetime of filter cartridges. Simon *et al.* (2007) studied the characteristics of reverse flow cleaning of baghouse filters supported by rigid rings. Various cleaning mechanisms and aerodynamic behaviors at different locations of fresh and used baghouse filters were discussed. It is found that the top section of a baghouse filter has low cleaning efficiency as compared with the other section of the filter (because of the close proximity to pulsing-jet flow). In the top section of filters gas flow actually permeated from the outside to the inside of a baghouse filter in the reverse pulsing-jet cleaning. The similar observation was also found in the cases of pleated filter cartridges. Lo *et al.* (2010a) and Yan *et al.* (2013) found that the top section of pleated filter cartridges were difficult to be cleaned because the peak cleaning pressure was low, resulting in the patchy cleaning of filter cartridges. The aforementioned issue has not been efficiently solved yet. Only limited researchers explored new methods for solving the patchy cleaning at the top section of pleated filter cartridges (Yan *et al.*, 2013).

Set pressure for the compressed gas tank and flow pulse duration for the reverse flow cleaning are two operational parameters which can be easily varied in filtration systems. Increasing the overpressure by increasing the tank pressure and extending the pulse duration have been proved to be efficient in enhancing the local cleaning efficiency. However, the disadvantages of increased tank pressure are (1) the increase of energy consumption for the cleaning operation, and (2) the potential increase of filter medium damage by excessive stresses.

To solve the patchy cleaning issue under the consideration of less energy consumption and minor/no tank pressure increase we proposed to clean filter cartridges via multiple pulsing jets, instead of one single pulsing jet typically applied in existed filtration system. The above-proposed cleaning mode is called in this work as the "reverse multi-pulsing jet" cleaning. Numerical modeling of transient flow and pressure fields under the reverse pulsing-jet cleaning (with single pulse) revealed that the effective cleaning time (considering the cleaning due to local mechanical stresses) was actually varied much at different locations of filter cartridges, especially at the top section of cartridges. In extreme cases, the effective cleaning times for the top and base sections of filter cartridges could be different by a factor of more than 1000 times. We thus hypothesized that multiple pulsing of reverse jet flow in the cleaning may result in better cleaning performance than single pulsing.

The objective of this work is thus to numerically investigate the quality of reverse flow cleaning via multiple pulsing schemes for pleated filter cartridges. A 3D transient model for pleated filter cartridges was developed to study the performance of proposed cleaning. Filter cartridges with V-shaped pleats were selected as model filter cartridges. In addition to the single pulsing scheme, the schemes with three other waveforms for the opening of the tank valve were also designed in this study. Notice that the total valve opening time for all studied waveform modes was kept the same.

NUMERICAL MODELING

Numerical Approach and Models

The Computational Fluid Dynamics (CFD) code (ANSYS CFX R.14, 2011) was applied in this study to calculate the flow and pressure fields in a single-unit filtration system under the reverse flow cleaning. The modeling solved unsteady Reynolds-averaged Navier-Stokes (N-S) equations for a single-phase flow. The element-based finite volume method with a high resolution scheme was applied to discretize the convection terms in the general transport equations (including N-S equations). The second-order backward Euler scheme was applied to the time-derivative terms in the equations. The pressure-coupled solver was used in ANSYS CFX to solve discretized equations.

Isothermal flow was assumed in the filter medium domain while the total energy was set in the fluid domain. The SST k-ω turbulent model with second-order accuracy was selected in this modeling with an automatic wall function. The turbulence flow model has been extensively validated for a wide range of flows and proved to have better performance than the standard k-ε model in various examples (Menter *et al.*, 2003). The marching step in time was set at 0.3 ms.

Fig. 1(a) shows the schematic diagram of a single-cartridge filtration system under this study. Also included in the same figure are filter cartridges with triangular pleats (shown in Fig. 1(b)). Filter cartridges with triangular pleats (given in Fig. 1) were considered in this study. The modelled filter cartridge was selected from one of three example cartridges studied in the work of Lo *et al.* (2010b). The thickness of filter media was assumed to be 0.8 mm. The wall thickness of the injection nozzle was given as 0.5 mm. Note that the diameter and length of modelled injection nozzle are also given in Fig. 1(a). The injection nozzle was placed along the axis of filter cartridges. No blow tubing was included in our model. Fig. 1(b) shows the definition of "outer" and "inner" surfaces of filter cartridges. The angles (θ and θ'), representing the geometric characteristics of a single pleat, were calculated by dividing 360° with the total number of pleats of studied filter cartridges.

Only a pleat element was considered in our modelling because of the circumferential symmetry of studied filter cartridges, nozzle arrangement and filtration system configuration. For simplicity clear filter cartridges were assumed in the majority of the modelling. Fig. 2 shows the schematic diagram of typical computational domain (with 30 copies). Only the flow and pressure fields during reverse flow cleaning were calculated.

ANSYS ICEM CFD R.14 was used to generate structured meshes in the computational domain. 3D hexahedral elements were used. The meshes near the surfaces of filter media and nozzle were further refined to ensure the y^+ (i.e., the dimensionless wall distance) of the first mesh layer adjacent

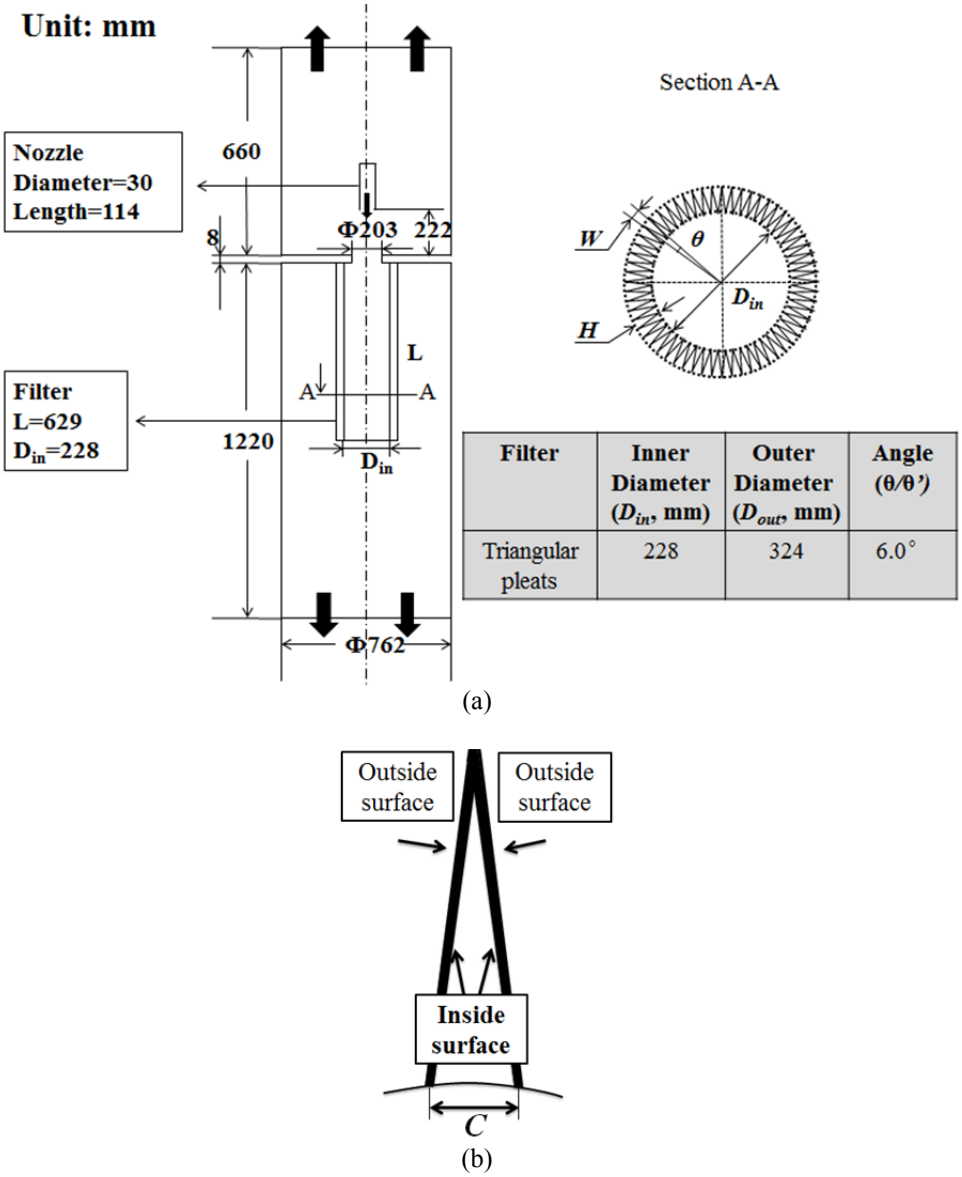

Fig. 1. Schematic diagram of studied filtration system having one pleated filter cartridge and injection nozzle (a) and the pleat shape of studied filter cartridge (b).

to walls is less than 1.0. The calculated meshes with encrypted meshes on the surface of filter media was ~0.1 million. In addition, the node number along the thickness of filter media was set to 16 to improve the meshing accuracy of medium domain.

Boundary Conditions

The total-pressure boundary condition was applied to one inlet of the computational domain and average static-pressure condition was applied to two outlets of the computational domain. In reality, once the cleaning is initiated, high-pressure gas from the pressured gas tank flows through a solenoid valve, a long flow distribution pipe to an injection nozzle. In this modelling, gas flow from the pressure tank to the inlet of injection nozzles was not included. Instead, it was simplified to apply a transient total-pressure distribution at the inlet of injection nozzle.

Four different waveforms for the transient total pressure at the nozzle inlet (shown in Fig. 3(a)) were investigated. They include the single pulsing mode (i.e., waveform 1, representing the mode typically used in industrial filtration systems) and three periodical pressure modes (i.e., waveforms 2, 3 and 4, respecting the multiple pulsing modes). The design of these waveforms was based on the data given in the work of Lo *et al* (2010b): when the tank pressure and pulse duration were set at 482,370 Pa and 350 ms, the measured highest total pressure and pulse duration at the nozzle inlet were 45 kPa and 0.5 s during air injection, respectively. Note that the peak total pressure and total pulse duration in all the modes are kept the same. The waveform 1 mode operation was selected as the reference. At the outlets of computational domain, one standard atmospheric pressure was applied as an average static pressure. The inlet static temperature and turbulence intensity were 300 K and 5%, respectively.

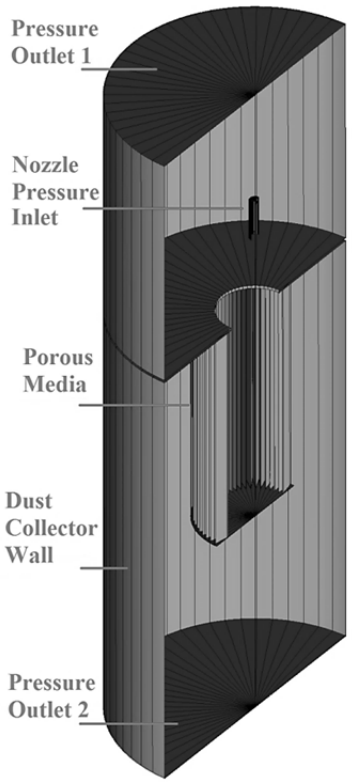

Fig. 2. Schematic diagram of a typical computational domain used in our study (shown in the figure is the 30 copies of actual computational domain).

The computational domain consisted of three sub-domains: two for flow in space and one for flow in porous media. Sub-domains of different physical types were joined together via the general grid interface (GGI) allowing the energy to flow through the interfaces. GGI permits the mis-matching of node location, element type, and surface extent and shape as well as flow physics.

Filter Media Models

Flow in filter media can be calculated by either a momentum loss model or full porous model included in ANSYS CFX (ANSYS Inc., 2011). In this study, porous filter media was assumed to be isotropic and a momentum loss model was selected to model the flow resistance characteristics of pleated filter media. Momentum source terms are used to model isotropic losses in isotropic porous media. The momentum losses in an isotropic porous media can be expressed as the following:

$$S_{M,x} = -\frac{\mu}{K_1}U_x - K_2\frac{\rho}{2}|U|U_x \tag{1a}$$

$$S_{M,y} = -\frac{\mu}{K_1}U_y - K_2\frac{\rho}{2}|U|U_y \tag{1b}$$

$$S_{M,z} = -\frac{\mu}{K_1}U_z - K_2\frac{\rho}{2}|U|U_z \tag{1c}$$

where K_1 and K_2 are the permeability and quadratic loss coefficient, respectively, which were given in the computation. U is the superficial velocity of filter media. The linear source term represents viscous loss and the quadratic term for inertial loss. In most cases, the linear term is dominant in pressure loss across porous media. The effect of porosity is accounted via this linear loss term. K_1 can be estimated from the Darcy's law (ASTM D737-04, 2012) and its general form is expressed as:

$$K_1 = -\frac{\mu}{\nabla p}U_0 \tag{2}$$

where ∇p is the pressure gradient across porous media, and μ is the dynamic viscosity of gas at the temperature of 300 K. The superficial velocity of porous media, U_0, is difficult to be calculated accurately, so Eq. (2) can be converted to another form:

$$K_1 = -\mu\frac{Q}{A}\frac{L}{\Delta p} \tag{3}$$

where A is the cross section area, Q is the total flow rate across porous media, L is the thickness of porous media in the flow direction, and Δp is the pressure drop across porous media. K_1 and K_2 was set to 2×10^{-12} m^2 and 1,000 m^{-1}, respectively (because of the coefficients enabling the matching of filter-testing data in the literature (Lo, 2006; Lo *et al.*, 2010a). A porosity of 0.99 was assigned to the medium subdomain to model the presence of medium structure existed in the cartridge filters. The deformation of filter media under the reverse pulse-jet process was not considered in this modeling.

RESULTS AND DISCUSSION

Because of cartridge structure and filter media the cleaning mechanism for removal of dust cake from pleated filter cartridges is believed not the same as that for baghouse filters. A literature review shows that the reverse airflow action (Koch *et al.*, 1996; Simon *et al.*, 2004), pressure drop and/or pressure acceleration (Lu and Tsai, 1996; Kanaoka and Kishima, 1999) and peak pressure (Li *et al.*, 2015; Yan *et al.*, 2015) have non-negligible roles for the dust removal via reverse flow cleaning. Different cleaning mechanisms may also exist from the top section to the base of filter cartridges (Simon *et al.*, 2007). The above-listed factors were often used in the literature as the criteria in determining the efficiency and quality of reverse flow cleaning.

In a standard single-pulsing jet cleaning, the top section of filter cartridges experiences reverse airflow cleaning action only for a very brief period of time (when the jet stream arrives at the top of filters). After the brief time period, the cleaning pressure quickly becomes negative in value, losing its cleaning effectiveness and, even worse, re-picking up dust particles which were previously unloaded. As shown in Fig. 4, at t = 2.7 ms (at a very initial moment), a powerful jet flow near the nozzle exit resulted in positive high

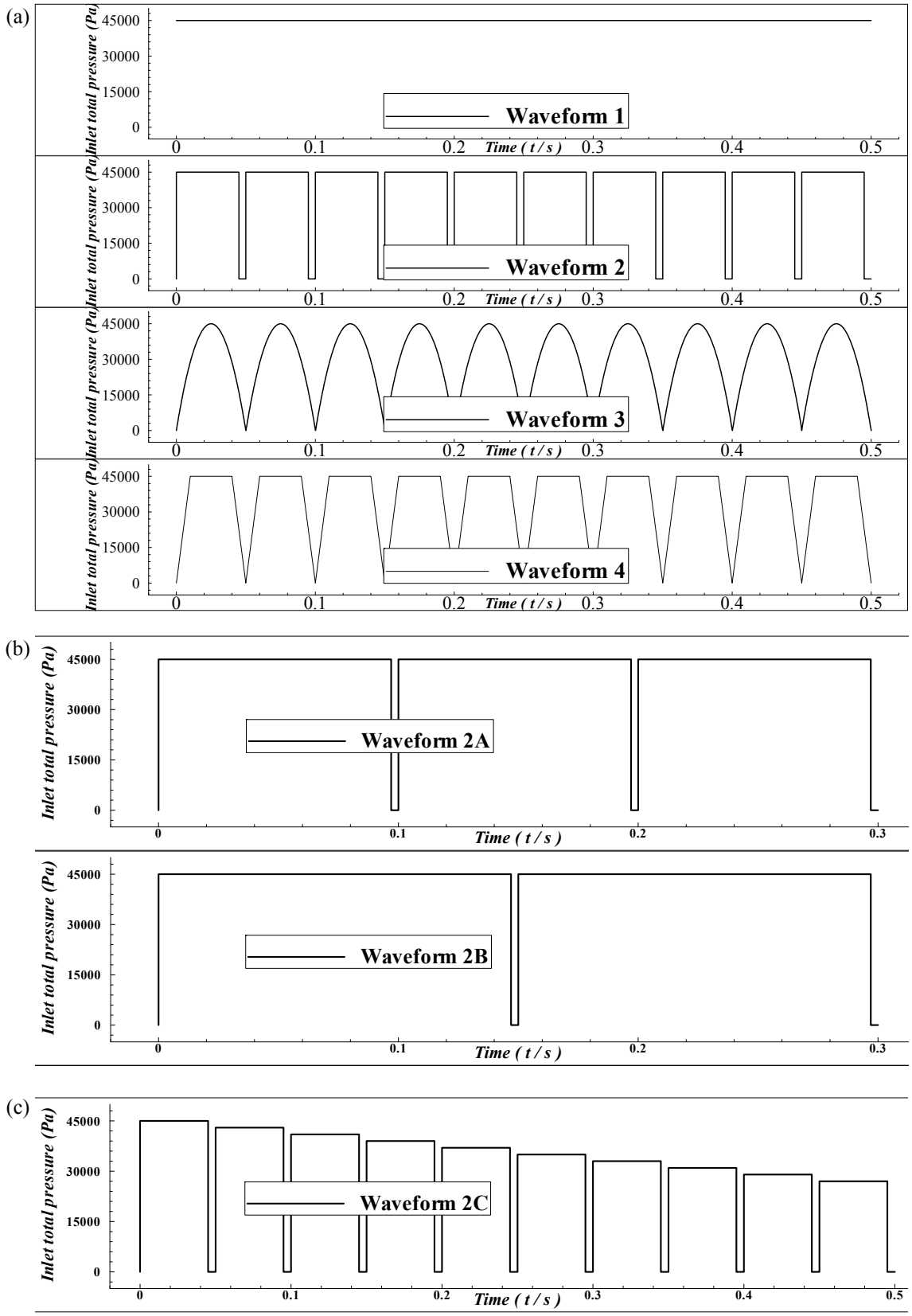

Fig. 3. Waveforms of total inlet nozzle pressure used in this study to investigate the feasibility of reverse flow cleaning via multiple pulsing jet operation: (a) are four different waveform shapes studied. Note that the single pulsing i.e., the waveform 1, is consider as the reference because it is a typical one applied in industrial filtration systems; (b) is for studying the effect of pulsing frequency on the quality of reverse flow cleaning; (c) is for the consideration of decreasing compressed gas tank pressure as the cleaning progress.

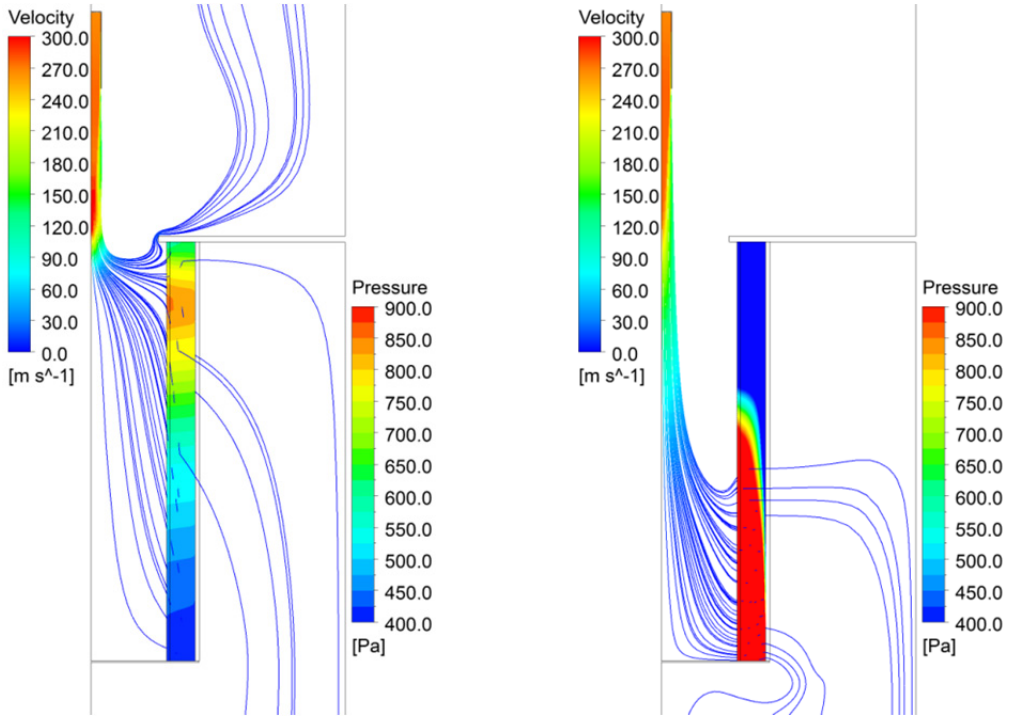

Fig. 4. Flow streamlines and static pressure in the studied filtration system at the time of 0.0027 and 0.3 s when operated in the cleaning cycle with the waveform 1.

pressure at the top section of the filter cartridge, driving gas flow to remove dust built-up on the outer surfaces of pleated filter cartridges. As the continuous development of jet flow, the positive high pressure zone moved to the base section of filter cartridges. At the same time, significant negative pressure appeared at the top section of cartridges as shown in Fig. 4 for t = 0.3s.

To improve the cleaning efficiency at the top section of filter cartridges, we proposed to operate the cleaning in a multiple pulsing mode. Fig. 5 shows the average pressure drop across pleated filter media over the entire filter surface as a function of time (t = 0~0.15 s). Compared with the single pulsing mode, the cleaning with multi-pulsing schemes kept the approximate pressure variation patterns as that of total pressures set at the nozzle inlet. The time variation of pressure drop in the multiple pulsing modes was divided into a series of pressure raise with no significant change of positive peak pressure. It is thus not possible to determine the cleaning in which waveform mode was better performed by the average pressure drop over the whole filter surface. To compare the performance of cleaning with various waveform schemes, we divided the whole filter cartridge (along the cartridge height) into ten sections (starting from the base section numbered as #1; shown in the side of Fig. 6). The peak pressure drop across pleated filter media and pressure acceleration are applied herein as the indicators for cleaning efficiency. Both high positive peak pressure drop and acceleration have beneficial roles in the reverse flow cleaning of pleated cartridge filters (Yan *et al.*, 2013, 2015). Notice that all the pressures discussed in the following are the static pressure drop across pleated filter media, not absolute pressure.

Fig. 6 shows the peak pressure gained at different sections of filter cartridges between t = 0.2s and t = 0.3s. For all three multi-pulsing waveform schemes, the peak pressure in the top section of filters, especially in the sections #7, #8, #9 and #10, obviously increased due to the multi-pulsing cleaning operation. Further, the peak pressure drop in the base sections of filter (i.e., the sections #1, #2, #3, #4 and #5) were also improved. As a result, the variation of peak pressure from the top to the bottom of filter cartridges was more gradual than that in single pulsing mode. The mechanism for the increase of peak pressure is in fact very different at the top and bottom of filter cartridge. Table 1 gives the ratio of average peak pressure drop at the sections #1, #2 and #3 when operated the cleaning in multiple pulsing modes (relative to that in the single-pulsing mode). The maximal peak pressure drop increase was 6.5% in the corresponding to the cleaning via the waveform 3 scheme. The increased peak pressure drop enhanced local cleaning mechanical stresses, expecting to result in better cleaning efficiency.

To further understand the transient characteristics of local pressure drop, the time dependent pressure variation at the sections #1, #2, #3, #8, #9 and #10 when pleated cartridges were cleaned via four waveform schemes are given in Fig. 7. For the pulsing modes with the waveforms 1 and 2, the pressure evolution has the similar trend during the initial pressurization because of the same total pressure setting at the nozzle inlet. For the cleaning modes with waveforms 3 and 4, higher peak pressure drop at the bottom sections and lower peak pressure drop at the top

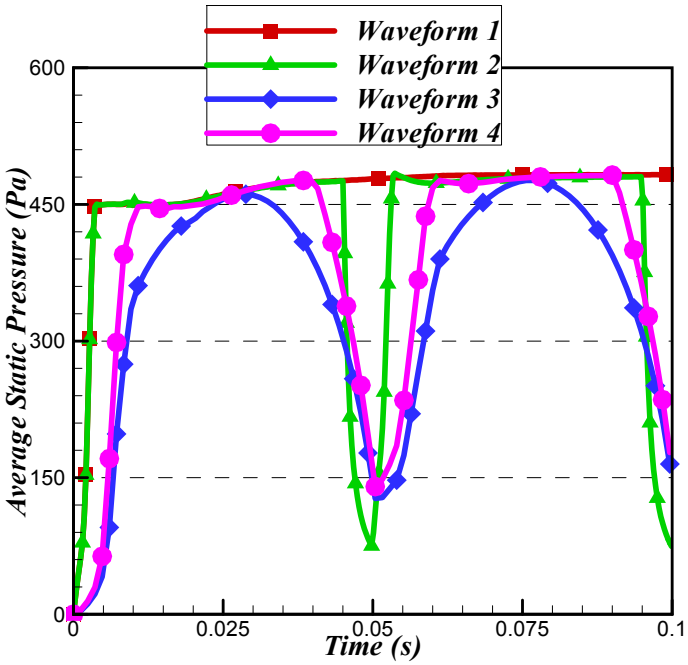

Fig. 5. Surface-averaged static pressure drop across pleated filter media as a function of time (t = 0–0.1 s) when filter cartridges were cleaned in the modes having the waveforms 1, 2, 3 and 4.

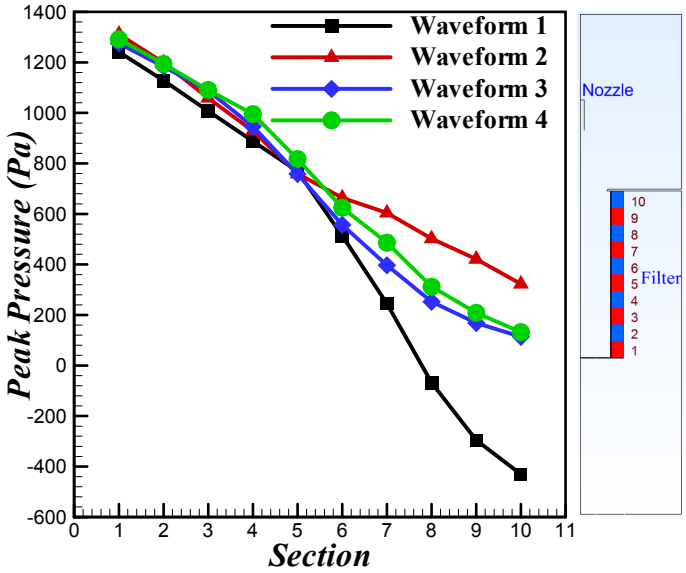

Fig. 6. Surface-averaged peak static pressure on filter surfaces at different sections of studied filter cartridges (t = 0.2–0.3 s). Also included is the schematic diagram of filter cartridge sections defined in this study.

sections of filter cartridges were observed during the initial pressurization. Note that the nozzle pressure rose in the modes of waveforms 3 and 4 is lower than that in the mode with waveforms 1 and 2 (as shown in Fig. 3). After the first pulse jet, the distribution characteristics of pressure waveforms remained similar in the following pulsing jets.

Also evidenced in Fig. 7, both a higher positive and lower negative peak pressure drops were observed in the top sections (i.e., the sections #8, #9 and #10) of filter cartridges, especially for the pulsing mode in the waveform 2. Significant pressure rise and fall events, in fact coincided with the opening and closing of tank valve. The fast pressurization is expected to result in quick local filter medium acceleration, resulting in improving the cleaning efficiency. It is surprising that the fast pressure acceleration was also observed at the bottom sections of filter cartridges. Different from the regular acceleration due to the medium movement, the present acceleration is stemmed from the multi-pulsing operation. The increased pressure drop and time of medium acceleration induced by the multi-pulsing operation are expected to efficiently restrain the re-attachment of dust previously unloaded.

Table 1. Increase of the surface-averaged peak pressure drop achieved in reverse flow cleaning when operated at multi-pulsing modes (relative to that when operated at single pulsing mode) at t = 0.2–0.3 second. The variables of "P_{a1}", "P_{a2}" and "P_{a3}" represent the average peak pressure drop at the sections #1, #2 and #3, respectively.

Increase (%)	P_{a1}	P_{a2}	P_{a3}
Waveform 2	5.4	4.9	2.9
Waveform 3	2.5	3.6	6.5
Waveform 4	3.8	4.5	6.1

It is worth noting that, observed in Fig. 7, the pressure evolution in the first pulsed jet is distinctly different from that in other following pulsed jets. To understand the above observation, Fig. 8 compares the transient distribution of static pressure for the pulsing mode with the waveform 2 at two selected time instances (t = 3 ms and 0.153 s). Two moments were selected because the jet flow just entered the filter cartridge at two different pulsing events. As evidenced in Fig. 8, the static pressure in the cartridge core at the time of 0.153 s is higher than that at the time of 3ms. At the ending of each pulsed jet, residual gas in the cartridge core had no sufficient time to be completely released. The formation of high-pressure zone is due to the interaction of residue gas left from the prior jet and the following jet. It is obvious that the mechanism to improve peak pressure at the bottom of filter cartridges has high correlation with the above interaction.

The pulsing frequency is expected to have impact on the performance of reverse flow cleaning. To investigate the pulsing frequency effect on the cleaning quality, two types of inlet total pressures at different pulsing frequencies (shown in Fig. 3(b)) were designed and applied as inlet boundary conditions in our modeling. Fig. 9 shows the distribution of time-dependent average pressure drop at the sections #1 and #2 of filter cartridges. With the reduced pulsing frequency, the peak pressures in the pulsing modes with the waveforms 2A and 2B were reduced as compared to that in the mode with the waveform 2. In particular, negative peak pressure drop in the section #10 of cartridges were reduced by nearly 50% and positive peak pressure in the section #1 of filters was very close to that obtained in the mode with the waveform 1. In addition, the reduced pressure in the section #10 of filters is expected to reduce medium acceleration. Pulsing the flow at high frequency is thus believed to result in better cleaning efficiency.

In reality, the tank pressure tends to reduce as the time progress in each cleaning cycle. To take the effect of total pressure decay in each cleaning phase into consideration, we revised the nozzle inlet pressure in our modeling to that designed in Fig. 3(c) (i.e., the waveform 2C). Given in Fig. 10 are the average pressure drops in the sections #1 and #10 of filter cartridges under the condition of tank pressure decreasing. At the higher tank pressure, the greater peak pressure drop at the cartridge base (i.e., the section #1) and greater pressure drop variation at the filter top (i.e., the section #10) at the jet initiation were observed. As the inlet tank pressure reducing, the above observation was gradually diminished. It is also found that the pressure variation at

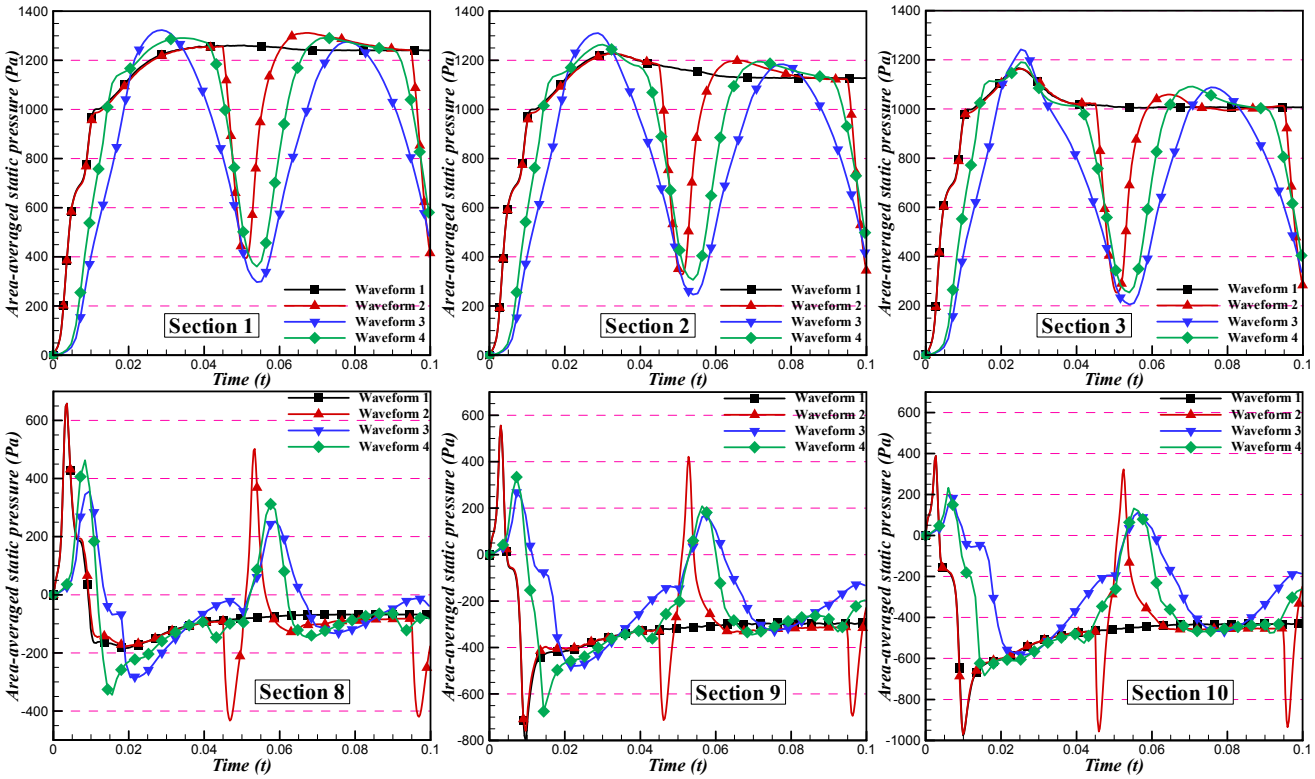

Fig. 7. Surface-averaged static pressure drop at the selected sections (#1, #2, #3, #8, #9, #10) of studied filter cartridges as a function of time under the cleaning with the modes having the waveforms 1, 2 3 and 4 (given in Fig. 3(a)).

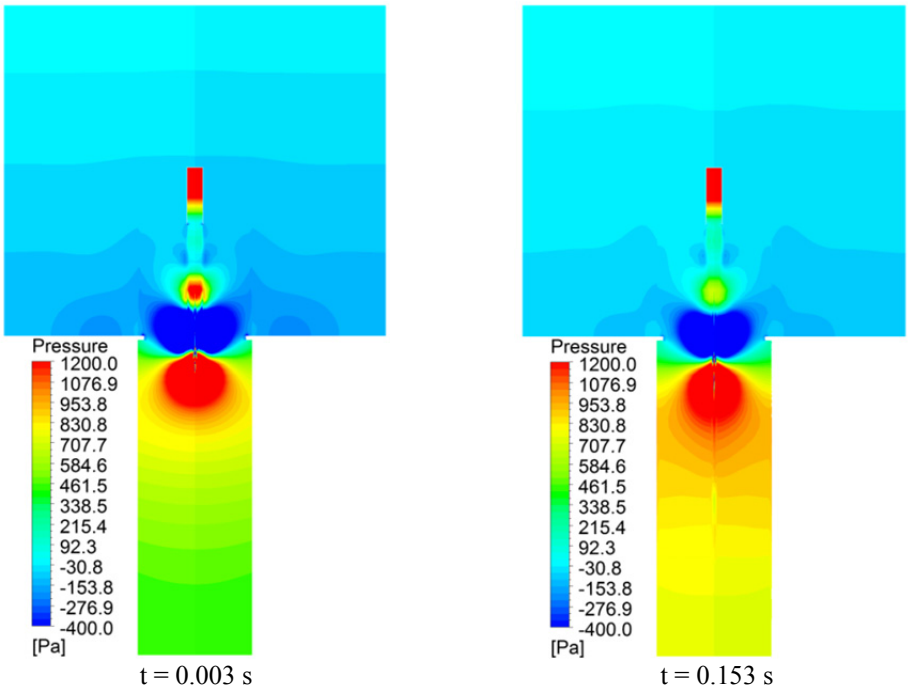

Fig. 8. Comparisons of pressure drop distributions at two selected time instances when filter cartridges was cleaned in the mode with the waveform 2 (left: the 1st jet pulsed at t = 0.003 s; right: the 4th jet pulsed at t = 0.153 s).

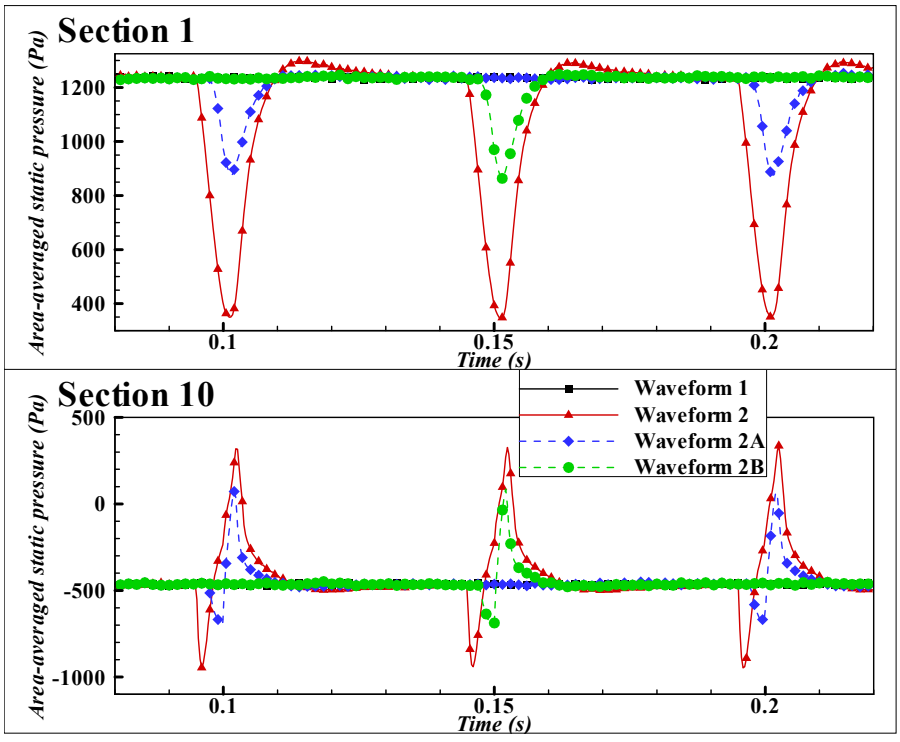

Fig. 9. Time-dependent surface-averaged static pressure drop at the section #10 of studied filter cartridges under the cleaning via the modes with the waveforms 1, 2 and 2A and 2B (showing the pulsing frequency effect).

low tank pressures was more gradual than that at high tank pressures, indicating the cleaning improvement due to the peak pressure is gradually reduced as the tank pressure decreasing.

To evaluate the performance of reverse flow cleaning in multi-pulsing modes under the consideration of dust cake removal during the cleaning process, a time-dependent permeability of filter media was applied to the porous medium model used in our modeling. According to the dust cake release behavior (as a function of time) observed

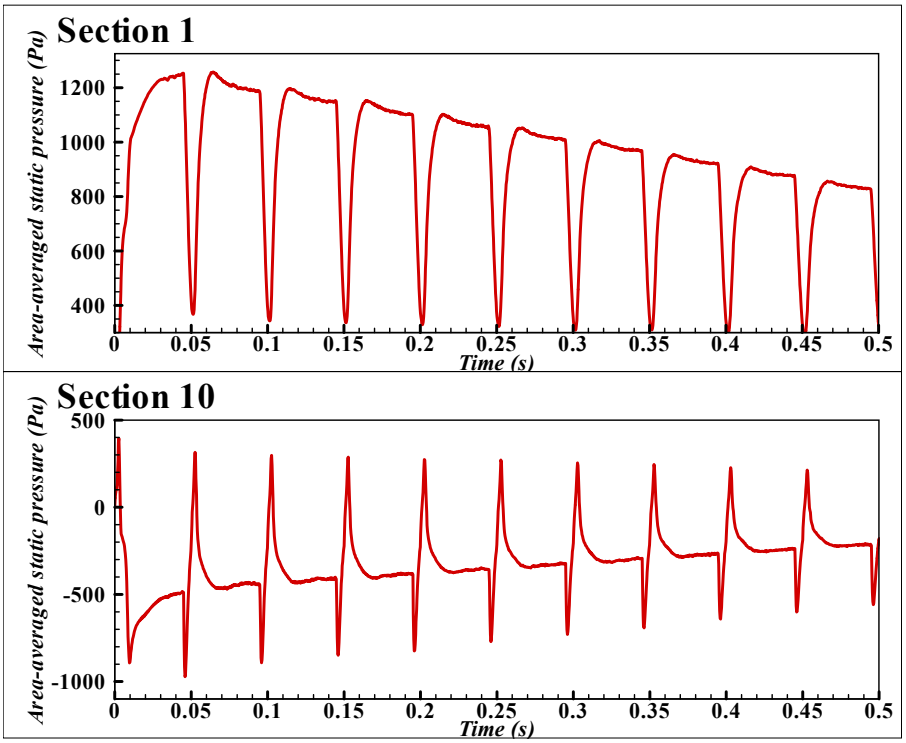

Fig. 10. Time-dependent surface-averaged static pressure at the sections #1 and #10 under the condition of decreasing tank pressure (Waveform 2C) (t = 0–0.5 s).

in the work of Ferer and Smith (1997) the time-dependent permeability of filter media during the cleaning phase was assumed in a logarithmic cake release mode (shown in Fig. 11). The initial permeability of porous media in the case of dense Al_2O_3 dust cake was set at 3.03692×10^{-14} m^2 and the final permeability in the case of loose dust cake was at 3.5×10^{-12} after an ideal cleaning (Lo, 2006). Fig. 12 shows the average static pressure drop in the sections #1 and #10 of filter cartridges when operating the cleaning in the modes of multiple pulsing (under the consideration of dust cake removal). As expected, the positive peak pressure drop at the cartridge base (i.e., the section #1) was increased during the operation of multiple jet-pulsing cleaning. Additionally, high medium acceleration due to multiple jet-pulsing was also evidenced. Note that the initial pressure rise in very initial cleaning phase (due to low filter permeability) was observed in this case. The improved effectiveness of multiple jet-pulsing cleaning is thus expected under the condition of dust cake removal.

CONCLUSIONS

Reverse flow cleaning (with single flow pulsing) is typically deployed in industrial filtration systems to re-generate filter media of pleated cartridges applied for collecting powder particles. The patchy cleaning at the top section of filter cartridges is often encountered in the practice. In this study we explored the feasibility of reverse flow cleaning via a multiple pulsing scheme in one cleaning cycle to improve the cleaning efficiency and quality of filter cartridges. A time-dependent 3D modelling of flow and pressure fields in a single-cartridge filtration system was carried out for this investigation. The effects of pulsing waveform and frequency on the quality of reverse flow cleaning of pleated filter cartridges were studied. Four waveforms and two frequencies of multi-pulsing mode operations were selected. It is concluded that the new cleaning operation using the multi-pulsing jets effectively improves the cleaning performance without the increase of compressed gas tank pressure. The multi-pulsing jet operation increases the number of cleaning actions and local medium acceleration at the top sections of filter cartridges. The operation further enhances the cleaning mechanical stress by raising the peak pressure drop at the bottom sections of filter cartridges. The improvement of cleaning efficiency could also be obtained via the increase of compressed gas tank pressure. However, the energy consumption of pumping gas to high pressure tank and increased potential to reduce the service lifetime of filter cartridges (due to medium damage under cleaning) would limit the use of tank pressure increase. The multi-pulsing operation studied herein could thus provide an easy solution for the cleaning quality improvement without the increase of compressed gas tank pressure.

Our study further found that, while the overall-surface-averaged peak pressure drop across pleated filter media remained unchanged, the average peak pressure drop at the bottom section of filter was 6.5% increased as compared to that under the cleaning with single jet-pulsing mode. Further, the multiple jet-pulsing mode of the waveform 2 provides better cleaning performance than those of the waveforms 3 and 4. It is because of the greater increase of positive peak pressure drop and medium acceleration at the

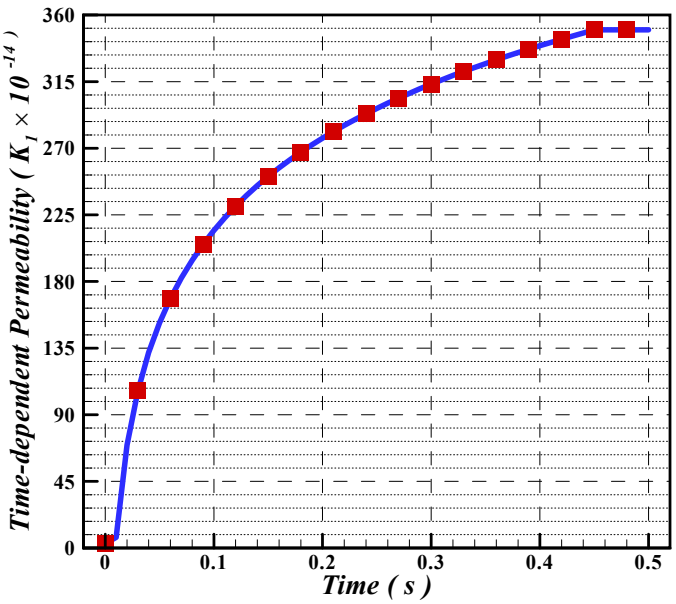

Fig. 11. Time-dependent permeability used to model dust removal from pleated filter cartridges during reverse pulse cleaning.

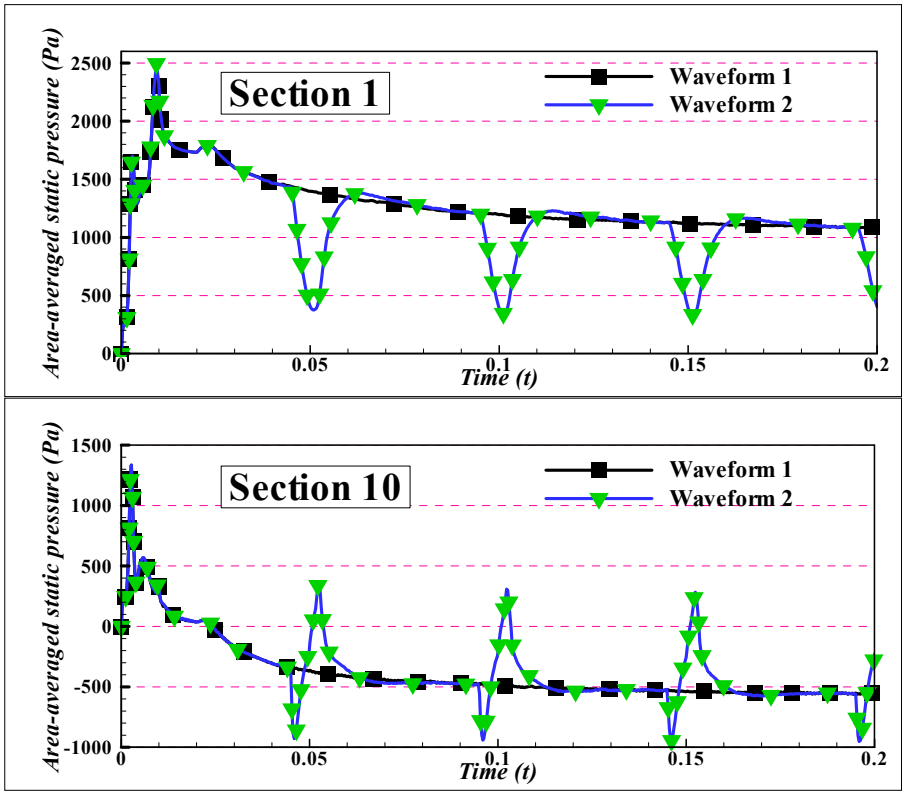

Fig. 12. Surface-averaged pressure drop at the sections #1 and #10 of studied filter cartridges as a function of time under the reverse flow cleaning in the waveforms 1 and 2 with the consideration of dust removal.

top sections of filter. The increase of peak pressure drop at the bottom section of filter cartridges was observed to correlate well with the interaction of residue gas, left from the former jet, and the following jet flow. The enhancement of medium acceleration at the top section of cartridges may disturb the re-attachment of cleaned dust, thus improving the cleaning quality. The high-frequency pulsing operation is believed to provide better cleaning performance because of the higher positive peak pressure drop in the cleaning. Further study indicated that the improvement of cleaning performance is achievable under the consideration of the tank pressure decrease and the time-dependent change of filter permeability during each cleaning cycle. It is also found that the pressure drop variation in the case at low

tank pressure setting was less than that in the case at high tank pressure setting, indicating the cleaning improvement attributed to the peak pressure drop is gradually reduced as the tank pressure decreasing.

ACKNOWLEDGEMENT

The authors are grateful to the support of the China Scholarship Council (CSC). The authors would also like to acknowledge the suggestions and assistances of Dr. Qiang Wang of Virginia Commonwealth University.

REFERENCES

Ahmadi, G. and Smith, D.H. (2002). Analysis of steady-state filtration and backpulse process in a hot-gas filter vessel. *Aerosol Sci. Technol.* 36: 665–677.

ANSYS Inc. (2011). ANSYS CFX Theory Guide, Release 14.0, Canonsburg. PA.

ASTM Int. (2012). Standard test method for air permeability of textile fabrics. ASTM D737-04. West Conshohocken, PA.

Bemer, D., Regnier, R., Morele, Y., Grippari, F., Appert-collin, J. and Thomas, D. (2013). Study of clogging and cleaning cycles of a pleated cartridge filter used in a thermal spraying process to filter ultrafine particles. *Powder Technol.* 234: 1–6.

Binnig, J., Meyer, J. and Kasper, G. (2009). Origin and mechanisms of dust emission from pulse-jet cleaned filter media. *Powder Technol.* 189: 108–114.

Calle, S., Contal, P., Thomas, D., Bemer, D. and Leclerc, D. (2002). Evolutions of efficiency and pressure drop of filter media during clogging and cleaning cycles. *Powder Technol.* 128: 213–217.

Calle, S., Contal, P., Thomas, D., Bemer, D., and Leclerc, D. (2004). Description of the clogging and cleaning cycles of filter medium. *Powder Technol.* 123: 40–52.

Chen, D. and Pui, D.Y.H. (1996). Optimization of pleated filter designs. *J. Aerosol Sci*. 27: 654–655.

Cheng, Y.H. and Tsai, C.J. (1998). Factors influencing pressure drop through a dust cade during filtration. *Aerosol Sci. Technol.* 29: 315–328.

Ferer, M. and Smith, D.H. (1997). A simple model of the adhesive failure of a layer: Cohesive effects. *J. Appl. Phys.* 81: 1737–1744.

Ji, Z., Shi, M. and Ding, F. (2004). Transient flow analysis of pulse-jet generation system in ceramic filter. *Powder Technol.* 139: 200–207.

Ji, Z., Li, H., Wu, X. and Choi, J. (2008). Numerical simulation of gas/solid two-phase flow in ceramic filter vessel. *Powder Technol.* 180: 91–96.

Kanaoka, C. and Kishima, T. (1999). Observation of the process of dust accumulation on a rigid ceramic filter surface and the mechanism of cleaning dust from the filter surface. *Adv. Powder Technol.* 10: 417–426.

Koch, D., Seville, J. and Clift, R. (1996). Dusk cake detachment from gas filters. *Powder Technol.* 86: 191–195.

Leith, D. and Ellenbecker, M.J. (1980). Theory for pressure drop in a pulse-jet cleaned fabric filter. *Atmos. Environ.* 14: 845–852.

Li, J., Li, S. and Zhou, F. (2015). Effect of cone installation in a pleated filter cartridge during pulse-jet cleaning. *Powder Technol.* 284: 245–252.

Li, Q., Zhang, M., Qian, Y., Geng, F., Song, J. and Chen, H. (2015). The relationship between peak pressure and residual dust of a pulse-jet cartridge filter. *Powder Technol.* 283: 302–307.

Lo L. (2006). Experimental study and numerical analysis for pleated filter cartridges in a pulse-jet cleaned dust collector. Ph. D. Thesis, University of Minnesota, Twin Cities.

Lo, L., Hu, S., Chen, D. and Pui D.Y.H. (2010a). Numerical study of pleated fabric cartridges during pulse-jet cleaning. *Powder Technol.* 198: 75–81.

Lo, L., Chen, D. and Pui, D.Y.H. (2010b). Experimental study of pleated fabric cartridges in a pulse-jet cleaned dust collector. *Powder Technol.* 197: 141–149.

Lu, H.C. and Tsai C.J. (1996). Numerical and experimental study of cleaning process of a pulse jet fabric filtration system. *Environ. Sci. Technol.* 30: 3243–3249.

Menter, F.R., Kuntz, M. and Langtry, R. (2003). Ten years of industrial experience with the SST turbulence model. In *Turbulence, Heat and Mass Transfer 4*, Hanjalic, K., Nagano, Y. and Tummers, M. (Eds.), Begell House, New York, pp. 625–632.

Novick, V.J., Monson, P. R. and Ellison, P. E. (1992). The effect of solid particle mass loading on the pressure drop of HEPA filters. *J. Aerosol Sci*. 23: 657–665.

Park, B.H., Lee, M., Jo, Y.M. and Kim, S.B. (2012). Influence of pleat geometry on filter cleaning in PTFE/glass composite filter. *J. Air Waste Manage. Assoc.* 62: 1257–1263.

Qian, Y., Bi, Y., Zhang, Q. and Chen, H. (2014). The Optimized relationship between jet distance and nozzle diameter of a pulse-jet cartridge filter. *Powder Technol.* 266: 191–195.

Simon, X., Thomas, D., Bemer, D., Calle, S., Regnier, R. and Contal, P. (2004). Influence of cleaning parameter on pulse-jet filter bag performance. *Filtration* 4: 253–260.

Simon, X., Chazelet, S., Thomas, D., Bemer, D. and Regnier, R. (2007). Experimental study of pulse-jet cleaning of bag filters supported by rigid rings. *Powder Technol.* 172: 67–81.

Yan, C., Liu, G. and Chen, H. (2013). Effect of induced airflow on the surface static pressure of pleated fabric filter cartridges during pulse jet cleaning. *Powder Technol.* 249: 424–430.

Yan, C., Zhang, M. and Lin, L. (2015). On-line pulse-jet cleaning of pleated fabric cartridge filters for collecting pesticides. *RSC Adv.* 59: 48086–48093.

Received for review, November 20, 2015
Revised, January 11, 2016
Accepted, January 23, 2016